



<b>Title</b>	<b>Aberration measurement using in-situ two-beam interferometry</b>
<b>Author(s)</b>	<b>Kirk, JP; Kunkel, G; Wong, AKK</b>
<b>Citation</b>	<b>Optical microlithography XIV, Santa Clara, USA, 27 February - 2 March 2001, v. 4346, p. 8-14</b>
<b>Issued Date</b>	<b>2001</b>
<b>URL</b>	<b><a href="http://hdl.handle.net/10722/46227">http://hdl.handle.net/10722/46227</a></b>
<b>Rights</b>	<b>Creative Commons: Attribution 3.0 Hong Kong License</b>

# Aberration measurement using in situ two-beam interferometry

J.P. Kirk  
IBM Microelectronics  
G. Kunkel  
Infineon Technologies  
A.K. Wong  
Hong Kong University

**Key words:** aberrations, blazed gratings, two beam interferometry, lens stability, surface relief images

## ABSTRACT

A reticle with phase-only blazed gratings of varying azimuthal orientations diffracts light into only two orders, 0 & +1, discretely illuminating a lens pupil. The image of each grating is a sinusoidal interference pattern and is recorded as a surface relief in a highly absorbing photoresist. The maximum image contrast occurs when focus is set such that the RMS wavefront error over the two beams is minimized. This maximum contrast vs focus is recorded by a CCD array mounted on a dark-field optical microscope and the aberrations are obtained from an analysis of this record. Repeatability of equivalent primary aberrations of less than  $0.001\lambda$  RMS are achieved and used to monitor lens stability.

## 1. INTRODUCTION

In order for the photolithographer to control his process it is essential that the condition of the lens at time of use be known. If the process was previously established using this lens, it may only be necessary to confirm if its condition has changed when trying to establish the cause of an observed process variation. If the process is yet to be established, a full description of the lens aberrations is needed to do a reliable process simulation of patterns intended for manufacturing. An in situ phase measuring interferometry, PMI, would answer both questions, but no such device is available and usually the last PMI data was taken prior to installation of the lens in the completed tool. Since then the tool was shipped, installed and frequently the lens is given a final adjustment so its current condition may not be that determined from the last PMI measurement.

In situ tests<sup>[1]</sup> are available ranging from those that simply test to see if the lens gives sufficient process latitude for a particular application to tests that attempt to duplicate PMI's ability to determine Zernike coefficients describing the aberrated wavefront. We describe improvements in a previously described technique<sup>[2]</sup> that uses a blazed grating reticle that illuminates the pupil in two beams and the image is recorded in highly absorbing photoresist<sup>[3]</sup> forming surface relief images that are measured with a conventional dark-field microscope. The result is a robust, precise and repeatable test that can be used as a simple monitor with minimal measurement or used as a detailed lens characterization requiring more measurement and analysis.

## 2. THEORY

Reticles can be designed that arbitrarily place the two beams within the pupil<sup>[4]</sup> but here we use a phase only blazed gratings, each period consists of line widths in the ratio of 1:2:1 with phases of 0:90:180 degrees. This grating does not diffract light into the -1 order, figure #1. It diffracts into higher orders, but by proper choice of grating period and partial coherence the higher orders are diffracted out of the lens NA so that the image will be a two beam interference of the zero and +1 orders. An image point at the center of a reference sphere that best matches the

converging wavefront is the focal point where contrast maximizes. It is shown analytically<sup>[5]</sup> that contrast will maximize for a value of defocus that minimizes the RMS wave front error over the regions of pupil illumination.

Different angular orientations of the grating will diffract the +1 order into different azimuthal positions in the pupil while the zero order reference beam remains centered in the pupil, figure #2. The test reticle consists of a set of gratings, each with an angular orientation incremented so the set has a range of orientations from zero to 360 degrees. In this way the diffracted +1 orders will sample the pupil in an annular ring with an NA radius of  $\lambda/\text{grating period}$ . If the lens has no aberrations, the best focus will occur at the same focal position for all gratings, that is regardless of the azimuthal region of the pupil used to form the image. If the lens has aberrations, figure #3, the best focus will change depending on how aberrations vary the wavefront as a function of azimuthal position of the +1 diffracted order, figure #4. For example, the value of best focus in the presence of coma will go through one cycle as the gratings rotate the first order through 360 degrees.

A set of Zernike polynomials, figure #5, describing wavefront aberrations has components with different azimuthal periods. Only coma has an azimuthal period of  $2\pi$ , astigmatism has fundamental period of  $\pi$ , 3-foil a period of  $2\pi/3$ , 4-foil  $\pi/2$ , etc. so the first harmonic in the function of focus vs grating angle is due solely to coma, the second harmonic is due to astigmatism, etc. The amplitude of these harmonics are directly proportional to the sum of the magnitudes of the corresponding aberration components. For example "X" coma, those with  $\cos\theta$  dependence, has an amplitude given by;

$$H1C_A = k_{A6}Z_6 + k_{A13}Z_{13} + k_{A22}Z_{22} + k_{A33}Z_{33} + \dots, \quad (1)$$

where  $H1C_A$  is the magnitude of the  $\cos\theta$  term in the first harmonic of focus vs azimuthal angle for the A exposure condition: H1, first harmonic; C,  $\cos\theta$  term; A, the exposure conditions, including grating period, partial coherence, NA, wavelength. The k's are proportionality constants relating each Zernike coefficient to the size of the harmonic in the function of focus vs azimuthal angle for the exposure conditions described by A. Similarly for the  $\cos 2\theta$  term in the second harmonic caused by the presence of astigmatism.

$$H2C_A = k_{A4}Z_4 + k_{A11}Z_{11} + k_{A20}Z_{20} + k_{A31}Z_{31} + \dots. \quad (2)$$

The values of the k's are found by simulation using a test set of Z's, and calculating the through focus images of the blazed gratings for the conditions described by A, finding the best focus vs azimuthal angle and calculating the amplitude of the harmonics.

These harmonics are experimentally measured as the Fourier transform of focus vs azimuthal angle as recorded by exposure in photoresist, figure #6. If only one exposure condition is used, it is not possible to determine how the various orders of aberration,  $Z_6$ ,  $Z_{13}$ ,  $Z_{22}$ ,  $Z_{33}$ , are contributing to the measured harmonic; the harmonic is a lumped parameter with all orders of the specific azimuthal aberration contributing. Therefore, when the harmonic is zero it doesn't necessarily mean that X coma is zero because the orders may simply sum to zero for this exposure condition. On the other hand, if  $H1C_A$  has a measured value, then the lens does have X coma and it is convenient to state the magnitude as an "equivalent primary coma" that will alone give the observed harmonic.

$$Z_6 = H1C_A / k_{A6}. \quad (3)$$

Now consider different exposure conditions, A,B,C,D,E, figure #7, each with a different grating period causing the pupil to be sampled at several different radii. The  $\cos\theta$  term of the first harmonic of focus vs azimuthal grating angle for each of these exposure conditions is given by:

$$\begin{bmatrix} H1C_A \\ H1C_B \\ H1C_C \\ H1C_D \end{bmatrix} = \begin{bmatrix} k_{A6} & k_{A13} & k_{A22} & k_{A33} \\ k_{B6} & k_{B13} & k_{B22} & k_{B33} \\ k_{C6} & k_{C13} & k_{C22} & k_{C33} \\ k_{D6} & k_{D13} & k_{D22} & k_{D33} \end{bmatrix} \times \begin{bmatrix} Z_6 \\ Z_{13} \\ Z_{22} \\ Z_{33} \end{bmatrix}. \quad (4)$$

Consider a hypothetical lens whose wavefront is fully described by a 37 term Zernike polynomial. Establish by simulation the k's for each exposure condition by determining the focus vs azimuthal angle for each condition and calculating the  $\cos \theta$  term of the first harmonic.

Using these k's and the harmonics measured from the resist images formed by this lens, the "equivalent four coma orders" of X coma that will cause the observed harmonics is given by;

$$\begin{bmatrix} Z_6 \\ Z_{13} \\ Z_{22} \\ Z_{33} \end{bmatrix} = \begin{bmatrix} k_{A6} & k_{A13} & k_{A22} & k_{A33} \\ k_{B6} & k_{B13} & k_{B22} & k_{B33} \\ k_{C6} & k_{C13} & k_{C22} & k_{C33} \\ k_{D6} & k_{D13} & k_{D22} & k_{D33} \end{bmatrix}^{-1} \times \begin{bmatrix} H1C_A \\ H1C_B \\ H1C_C \\ H1C_D \end{bmatrix}. \quad (5)$$

This calculation is then done for the cos and sine terms of the first four harmonics of focus vs azimuthal angle giving the 28 Zernike coefficients; coma, astigmatism, 3 foil, and 4 foil. For this lens, within the limit of measurement noise, the coefficients so measured will be correct coefficients of the Zernike polynomial expansion of the wavefront.

In practice, the image in the photoresist from which the harmonics are derived is formed with higher order aberrations that couple into the first four orders of Zernike coefficients obtained from the above calculation. In the same way as we identified an "equivalent primary coma" from one exposure condition we can identify an "equivalent four coma orders" from analysis of the multiple exposure conditions. While these equivalent aberrations are the ones that would cause the observed variations in the images of blazed gratings, caution must be observed in using them to predict the images of other types of objects. In any case, they help sort out which of the low order terms are present in the lens and these terms have values only when aberrations are present. In this way they give a more detailed accounting of lens quality.

### 3. APPLICATION

The reticle we used consists of rows of 16 squares, 29 microns on a side, containing a phase gratings each incremented by 22.5 degrees and the columns are surrounded by opaque chrome. In this way the, the pupil is sampled in equal azimuthal increments from 0 to 237.5 degrees. This pattern is repeated 4 times within a column at periods of 1350, 720, 480, and 360nm enabling azimuthal sampling a different radii. The entire reticle is filled with columns separated by 500 microns so 17 micro-steps of 29 microns can be done, as the focus is being incremented, before images overlap.

One field of exposures consists of a through focus sequence of 17 exposures, after each exposure the wafer in moved 29 microns. The resulting surface relief grating is then viewed with a dark-field microscope where the best focus, greatest modulation, appears brightest. This is repeated at different fields with focus increments of 50, 150, 200, 250 and 300nm to capture both the depth of focus for the different grating periods and focal variations caused by aberrations. I-line photoresist<sup>[6]</sup> used to record surface relief images at 248nm wavelength and 248nm photoresist<sup>[7]</sup> is use to record exposures at 193nm.

A dark-field microscope with a CCD array records the intensity of diffraction from the relief images, the maximum indicating best focus, figure #8. This record of best focus vs azimuthal angle is Fourier analyzed to separate the harmonics; coma, astigmatism, 3-foil, and 4-foil.

An example of using this method to track the condition of a particular lens is recorded in the following figures. A single grating period 720nm was used so only "equivalent primary" aberrations are recorded at several locations along the center of the lens field. The measured aberrations are plotted as vectors, figure #9, to make it is easy to see the across field variation of the four azimuthal aberrations (Note: spherical aberration is obtained from a 3 beam interferometer<sup>[8]</sup>). The measurement was repeated five times over a period of 35 days and the "equivalent primary" coma for each day is plotted in Figure #10. Over this time period the mean value of X coma ( $\cos \theta$ ) varies within a range of  $\pm 0.0002 \lambda$  RMS and the Y coma ( $\sin \theta$ ) within a range of  $\pm .002 \lambda$  RMS. The mean value of X

& Y coma is plotted in figure #11 where their relative stability is compared. The error associated with and individual measurement is estimated from the combined data of figure #9. The offsets and linear across field variations are removed for each plot, figure #12, and the combined deviations of each field point about its mean is found to have standard deviation of  $0.0008 \lambda$  RMS.

Separating the higher order aberration terms requires measurement of the azimuthal focal variation at several different radii. It is difficult to manually acquire the images of the higher frequency gratings that must be measured with high numeric aperture microscope objectives needed to capture the light diffracted at large angles from the relief images. This practical difficulty is resolved by the installation of microscope with automated data acquisition.

#### 4. SUMMARY

We have presented a robust method of monitoring lens condition using a two beam interferometer formed by a blazed grating test reticle. Using highly absorbing photoresists and measuring with an optical microscope, repeatability of better than 0.001 waves RMS is achieved, enabling tracking of lens changes before they become significant detractors in a manufacturing process. Manual measurement of "equivalent primary" aberrations at 20 field positions can be done in less than 2 hours. With an automated microscope, the time from test exposure to display of a full higher order analysis will be a few minutes.

#### ACKNOWLEDGMENTS

The authors acknowledge the support of Alek Chen in his commitment to monitor tools using the methods reported here and Robert Dogga who exposed the wafers and made the measurements.

#### REFERENCES

- [1] J.P. Kirk, "Review of photoresist based lens evaluation methods", Proc. SPIE, vol. 4000, p. 2 (2000)
- [2] J.P. Kirk, C.P. Proglor, "Application of blazed gratings for determination of equivalent primary azimuthal aberrations", Proc. SPIE, vol. 3679, p. 70 (1999)
- [3] J.P. Kirk, M.S. Hibbs, "DUV diagnostics using continuous tone photoresist", SPIE Vol. 1463, pp. 575, 1991
- [4] A.E. Rosenbluth, et al., "Optimum mask and source patterns to print a given shape", SPIE, 4346-49, 2001
- [5] A.K. Wong, analytic proof available on request.
- [6] THMR-IP3250 LB manufactured by Ohka America Inc.
- [7] UV82 Positive DUV photoresist manufactured by Shipley Inc.
- [8] J.P. Kirk, "Detection of focus and spherical aberration by use of a phase grating", SPIE 4346-141, 2001

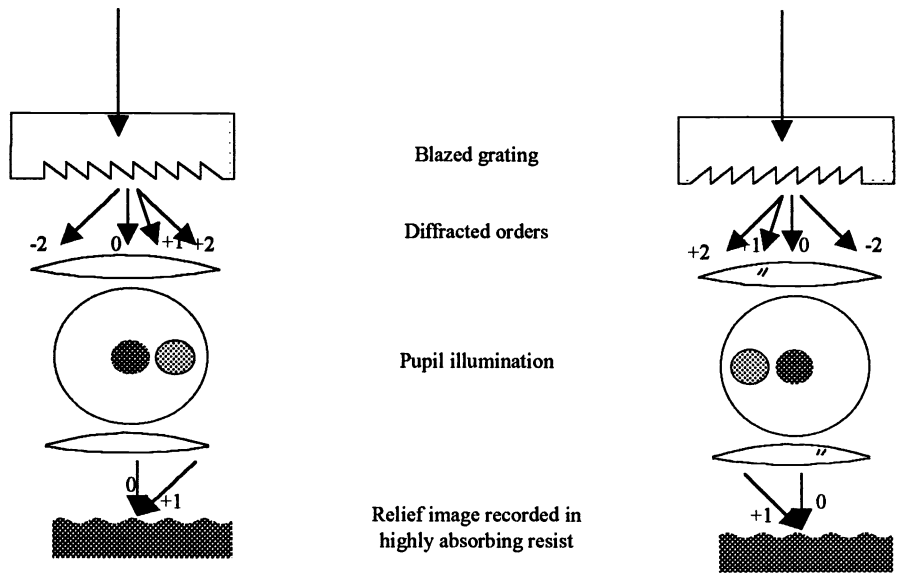


Figure #1. Blazed grating having no  $-1$  diffraction order. Higher orders are outside the lens collection NA.

Figure #2. Blazed grating rotated 180 degrees. Different region of lens used for image formation.

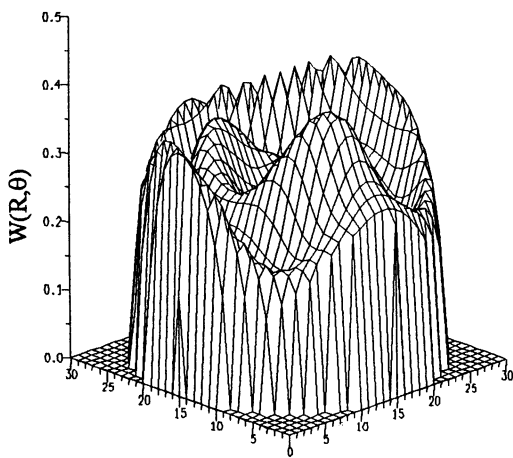


Figure #3. Typical aberrations found in a photolithography lens.

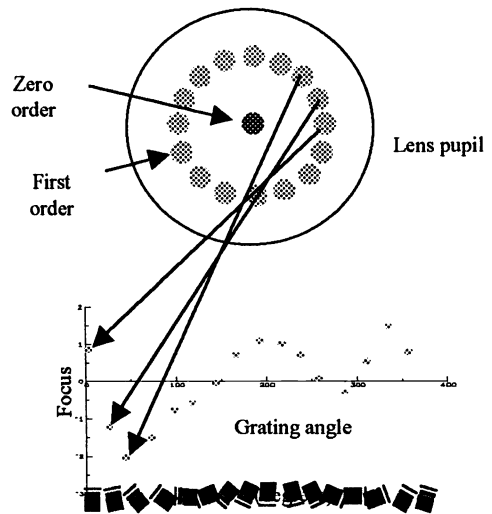


Figure #4. Focus as a function of pupil region illuminated.

$$\begin{aligned}
W(R, \theta) = & Z1 \times R \cos \theta & + Z18 \times (5R^2 - 4R^3) \cos 3\theta \\
& + Z2 \times R \sin \theta & + Z19 \times (5R^2 - 4R^3) \sin 3\theta \\
& + Z3 \times (2R^2 - 1) & + Z20 \times (15R^4 - 20R^4 + 6R^2) \cos 2\theta \\
& + Z4 \times R^2 \cos 2\theta & + Z21 \times (15R^4 - 20R^4 + 6R^2) \sin 2\theta \\
& + Z5 \times R^2 \sin 2\theta & + Z22 \times (35R^4 - 60R^4 + 30R^2 - 4R) \cos \theta \\
& + Z6 \times (3R^2 - 2R) \cos \theta & + Z23 \times (35R^4 - 60R^4 + 30R^2 - 4R) \sin \theta \\
& + Z7 \times (3R^2 - 2R) \sin \theta & + Z24 \times (70R^4 - 140R^4 + 90R^4 - 20R^2 - 1) \\
& + Z8 \times (6R^4 - 6R^2 + 1) & + Z25 \times (R^3) \cos 5\theta \\
& + Z9 \times (R^3) \cos 3\theta & + Z26 \times (R^3) \sin 5\theta \\
& + Z10 \times (R^3) \sin 3\theta & + Z27 \times (6R^4 - 5R^4) \cos 4\theta \\
& + Z11 \times (4R^4 - 3R^2) \cos 2\theta & + Z28 \times (6R^4 - 5R^4) \sin 4\theta \\
& + Z12 \times (4R^4 - 3R^2) \sin 2\theta & + Z29 \times (21R^7 - 30R^7 + 10R^2) \cos 3\theta \\
& + Z13 \times (10R^5 - 12R^5 + 3R) \cos \theta & + Z30 \times (21R^7 - 30R^7 + 10R^2) \sin 3\theta \\
& + Z14 \times (10R^5 - 12R^5 + 3R) \sin \theta & + Z31 \times (56R^9 - 105R^9 + 60R^4 - 10R^2) \cos 2\theta \\
& + Z15 \times (20R^6 - 30R^6 + 12R^2 - 1) & + Z32 \times (56R^9 - 105R^9 + 60R^4 - 10R^2) \sin 2\theta \\
& + Z16 \times (R^4) \cos 4\theta & + Z33 \times (126R^9 - 280R^9 + 210R^2 - 60R^2 + 5R) \cos \theta \\
& + Z17 \times (R^4) \sin 4\theta & + Z34 \times (126R^9 - 280R^9 + 210R^2 - 60R^2 + 5R) \sin \theta \\
& & \dots
\end{aligned}$$

Figure #5. Zernike polynomial representation of a wave front. Note: The only contributor to the first harmonic are coma terms.

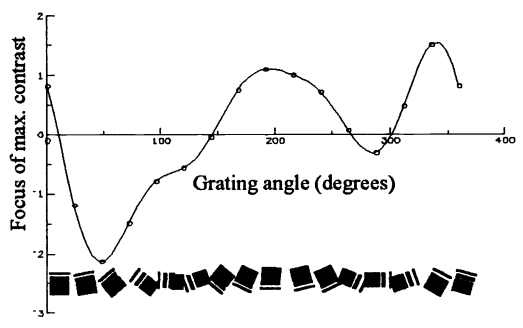


Figure #6. Focus vs azimuthal grating angle. FFT of this curve gives the harmonics that are related to the aberrations.

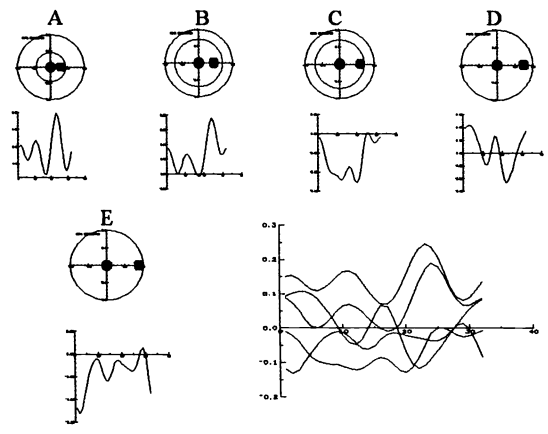


Figure #7. Focus vs azimuthal angle for 5 exposure conditions each sampled at different radii.

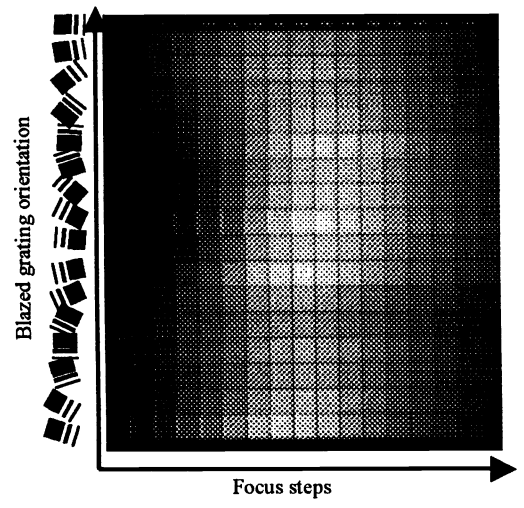


Figure #8. Dark-field image of the surface relief formed by micro-stepping the blazed grating through focus.

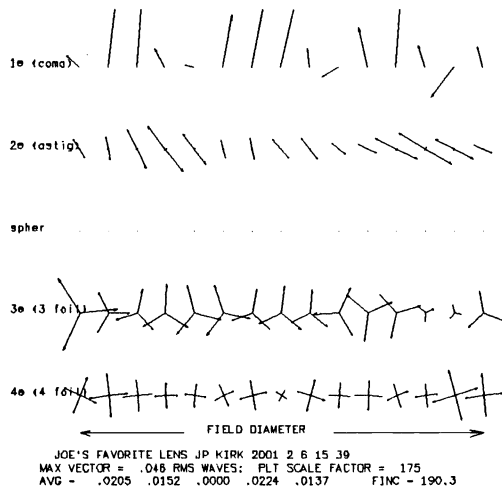


Figure #9. Vector plot of the first 4 azimuthal aberrations as a function of field position.

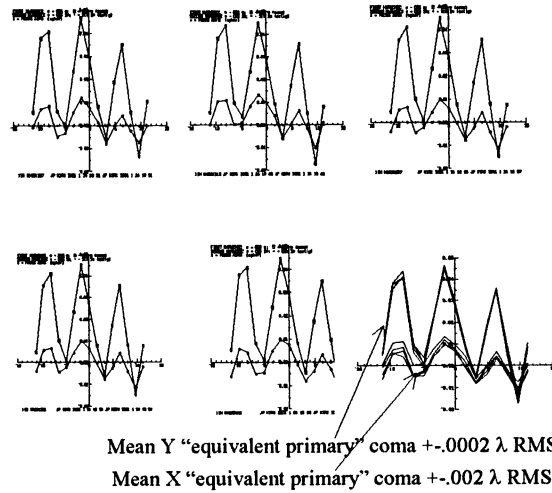


Figure #10. 5 repeated measurement of X and Y coma over a period of 35 days.

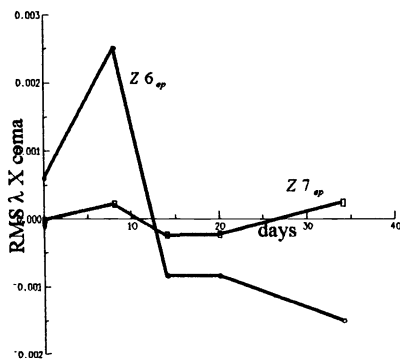


Figure #11. Wafer average X & Y "equivalent primary" coma over a period of 35 days.

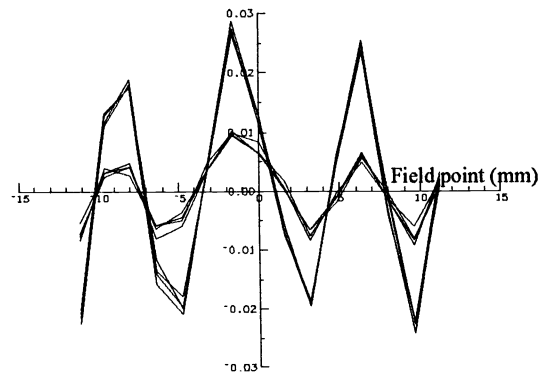


Figure #12. Over a period of 35 days Standard deviation = 0.00083  $\lambda$  RMS.